Published in final edited form as:
Nature. ; 482(7384): 237–240. doi:10.1038/nature10750.

G protein-coupled receptor inactivation by an allosteric inverse-agonist antibody

Tomoya Hino[1,2,*], **Takatoshi Arakawa**[1,2,*], **Hiroko Iwanari**[3,*], **Takami Yurugi-Kobayashi**[1,2,*], **Chiyo Ikeda-Suno**[1,2], **Yoshiko Nakada-Nakura**[3,4], **Osamu Kusano-Arai**[3,5], **Simone Weyand**[1,6,7,8], **Tatsuro Shimamura**[1,2], **Norimichi Nomura**[1,2], **Alexander D. Cameron**[1,6,7,8], **Takuya Kobayashi**[1,2], **Takao Hamakubo**[3], **So Iwata**[1,2,6,7,8,9], and **Takeshi Murata**[1,2,9,10]

[1]Iwata Human Receptor Crystallography Project, ERATO, Japan Science and Technology Agency, Yoshidakonoe-cho, Sakyo-ku, Kyoto 606-8501, Japan

[2]Department of Cell Biology, Graduate School of Medicine, Kyoto University, Yoshidakonoe-cho, Sakyo-ku, Kyoto 606-8501, Japan

[3]Department of Molecular Biology and Medicine, Research Center for Advanced Science and Technology, The University of Tokyo, 4-6-1 Komaba, Meguro-ku, Tokyo 153-8904, Japan

[4]Perseus Proteomics Inc, 4-7-6 Komaba, Meguro, Tokyo 153-0041, Japan

[5]Institute of Immunology Co. Ltd., 1-1-10 Koraku, Bunkyo, Tokyo 112-0004, Japan

[6]Division of Molecular Bioscience, Membrane Protein Crystallography Group, Imperial College London, Exhibition Road, London SW7 2AZ, UK

[7]Diamond Light Source, Harwell Science and Innovation Campus, Chilton, Didcot, Oxfordshire OX11 0DE, UK

[8]Research Complex at Harwell, Rutherford Appleton Laboratory, Harwell Oxford, Didcot, Oxon OX11 0FA, UK

[9]Systems and Structural Biology Center, RIKEN, 1-7-22 Suehiro-cho Tsurumi-ku, Yokohama 230-0045 Japan

[10]Department of Chemistry, Graduate School of Science, Chiba University, 1-33 Yayoi-cho, Inage, Chiba 263-8522, Japan

Abstract

Correspondence and requests for materials should be addressed to T.M. (t.murata@faculty.chiba-u.jp), S.I. (so_iwata@mac.com), T. Hamakubo (hamakubo@lsbm.org), or T.K. (t-coba@mfour.med.kyoto-u.ac.jp)..
*These authors contributed equally to this work.

Author Information. Atomic coordinates and structure factors for the A_{2A}AR-Fab structure have been deposited in the Protein Data Bank under the accession codes 3VG9 (2.7 Å data) and 3VGA (3.1 Å data).

Author Contributions. S.I. and T.M. designed the original research project. T.Y.-K. and T.K established the A_{2A}AR expression and purification protocols. T. Hino and C.I.-S. expressed, purified, and characterised the receptor. H.I., Y.N.-N., O.K.-A., and T. Hamakubo performed the immunisation, selection, and isolation of antibodies. T. Hino, T.A., and C.I.-S. purified and characterised antibodies. N.N. sequenced antibodies. T. Hino, T.A., and T.S. purified and crystallised the receptor-Fab fragment complex. S.W., A.D.C., and S.I. performed data collection. T. Hino solved and refined the structure. T. Hino, S.I., and T.M. wrote the manuscript and all authors provide editorial input. The project was managed by T. K., T. Hamakubo, S.I. and T.M.

Full Methods and any associated references are available in the online version of the paper at www.nature.com/nature.

Supplementary Information is linked to the online version of the paper at www.nature.com/nature.

The authors declare no competing financial interests.

Europe PMC Funders Author Manuscripts

G protein-coupled receptors (GPCRs) are the largest class of cell-surface receptors, and these membrane proteins exist in equilibrium between inactive and active states.[1-13] Conformational changes induced by extracellular ligands binding to GPCRs result in a cellular response through the activation of G-proteins. The A_{2A} adenosine receptor (A_{2A}AR) is responsible for regulating blood flow to the cardiac muscle and is important in the regulation of glutamate and dopamine release in the brain.[14] In this study, we have successfully raised a mouse monoclonal antibody against human A_{2A}AR that prevents agonist but not antagonist binding to the extracellular ligand-binding pocket. The structure of the A_{2A}AR-antibody Fab fragment (Fab2838) complex reveals that the fragment, unexpectedly, recognises the intracellular surface of A_{2A}AR and that its complementarity determining region, CDR-H3, penetrates into the receptor. CDR-H3 is located in a similar position to the G-protein C-terminal fragment in the active opsin structure[1] and to the CDR-3 of the nanobody in the active β_2 adrenergic receptor structure[2] but locks the A_{2A}AR in an inactive conformation. These results shed light on a novel strategy to modulate GPCR activity.

The GPCR structures in an inactive conformation solved recently[3-12] largely advance our understanding of the molecular signalling mechanisms of the receptors. The first details of GPCR activation were provided by the structure of bovine opsin in an active conformation complexed with a G-protein C-terminal peptide (GαCT)[1]. Most recently, Kobilka and colleagues obtained the crystal structures of β_2AR in an active state with a camelid antibody fragment (nanobody, Nb80)[2] and with a heterotrimeric Gs-protein[13]. In these structures, the complementarity-determining region (CDR-3) of Nb80 and C-terminal α-helix of α subunit (Gαs) of Gs-protein were located in the same pocket as for GαCT in the opsin structure. They showed that Nb80 and Gs protein change the conformational equilibrium of β_2AR toward the active state in a similar manner, thereby substantially increase their agonist affinities[2,13].

A_{2A}AR is responsible for regulating blood flow to the cardiac muscle and is important in the regulation of glutamate and dopamine release in the brain[14]. Caffeine is a well-known antagonist of this receptor. Strong epidemiological evidence indicates that coffee drinkers have a lower risk of Parkinson's disease[15]. The structure of A_{2A}AR has been reported[9,16] as a complex with both an antagonist (ZM241385) and an agonist (UK-432097). These structures reveal the molecular framework of the receptor; however, in both cases the intracellular loop 3 (ICL3), critical for G-protein binding, has been replaced by T4-lysozyme (T4L).

Here, we report the crystal structure of A_{2A}AR with complete ICL3 in complex with a mouse monoclonal-antibody Fab-fragment, Fab2838. A_{2A}AR was expressed in *Pichia pastoris* and the antibody was raised to the purified receptor with antagonist (ZM241385) bound using the conventional mouse-hybridoma system combined with improved immunisation and screening methods (for details, see Methods). Fab2838, a Fab fragment generated from one (IgG2838) of the obtained antibodies completely inhibited binding of the agonist [^{3}H]-NECA but did not affect binding of the antagonist [^{3}H]-ZM241385 (Fig. 1a,d and Supplementary Fig. 2). The results were confirmed by competition binding assays (for details, see Supplementary Discussion and Fig. 1). These findings suggest that Fab2838 induces an inactive conformation, (*i.e.* to which agonist cannot bind) of the A_{2A}AR ligand-binding pocket without blocking the ligand-binding site.

We crystallised A_{2A}AR with Fab2838 in the presence of ZM241385 and solved the structure at a resolution of 2.7 Å (Supplementary Table 2). Since the occupancy of ZM241385 in the structure was low for unknown reasons, we repeated the experiments and obtained a higher occupancy structure at 3.1 Å (Supplementary Table 2 and Supplementary Fig. 3 and 4). Except for the occupancy of the ligand, the two structures are almost identical (RMSD of Cα; 0.57 Å) (Supplementary Table 2). ZM241385 occupies the ligand-binding pocket on the

extracellular side by making hydrophobic interactions with F168$^{5.29}$ and I274$^{7.39}$, and hydrogen-bonds with N253$^{6.55}$ as observed in the A_{2A}AR-T4L structure (Supplementary Fig. 4). While the overall structure of A_{2A}AR in the A_{2A}AR-Fab2838 complex is similar to that of the T4L construct (PDB; 3EML) (RMSD of Cα; 0.85 Å), there is a major difference around the intracellular portions of helices V and VI, which are connected by ICL3, where T4L is inserted in A_{2A}AR-T4L (Supplementary Fig. 5). In our structure, ICL3 forms two regular helices, effectively continuations of helices V and VI respectively, connected by a short turn (Supplementary Fig. 6a).

The A_{2A}AR–Fab2838 structure has a modified 'ionic lock' where E228$^{6.30}$ (helix VI) and R102$^{3.50}$ of the D(E)RY motif (helix III) interact *via* a water molecule (W1; Fig. 2c,d). In the inactive bovine rhodopsin structure, the equivalent residues form a direct salt-bridge[3] (Supplementary Fig. 7). R102$^{3.50}$ of A_{2A}AR-Fab2838 forms salt-bridges/hydrogen-bonds with D101$^{3.49}$, Y112 in ICL2 and T41$^{2.39}$ as observed in the A_{2A}AR-T4L structure (Supplementary Fig. 5b). Because of the insertion of the water molecule, E228$^{6.30}$ shifts towards the cytoplasmic space, as compared to the equivalent residue in rhodopsin (E247$^{6.30}$), resulting in the formation of a salt bridge with R220 in the short helical turn of ICL3. This interaction may be important in the formation of the helical structure in ICL3. The 'ionic lock' has not been observed in the crystal structures of other inactive GPCRs[6-11], including A_{2A}AR-T4L, except for the D3 dopamine receptor[12]. This may be because the ICL3s in the other structures were modified to stabilise the protein. While this manuscript was in review, the crystal structures of thermostabilised A_{2A}AR mutants with native ICL3 were published[17,18]. The antagonist-bound inactive structures have the 'ionic lock'[18]. Thus, the 'ionic lock' of A_{2A}AR seems to stabilise the inactive conformation of the protein, which is why the receptor has a low basal activity.

Fab2838 binds on the intracellular side of the receptor (Fig. 2a). CDR-H3 of Fab2838 is unusually long and penetrates into a pocket formed by helices II, III, VI and VII (Fig. 2b). CDR-H3 interacts with the surrounding helices by forming 6 hydrogen bonds and 8 van der Waals contacts (Fig. 2c,d). The most extensive interactions are with helix II (mainly through hydrogen bonds) and helix VI (mainly through van der Waals contacts). In addition, a hydrogen-bond network including 2 water molecules is observed between CDR-H3 and helices III and VI (Fig. 2c,d). This hydrogen-bond network together with the van der Waals interactions seem to stabilise the modified 'ionic lock' interaction between E228$^{6.30}$ (helix VI) and R102$^{3.50}$ (helix III) discussed above. Other CDRs further stabilise the A_{2A}AR–Fab2838 complex by forming 14 hydrogen bonds with helices VI and VIII and ICLs 1, 2, and 3 (Fig. 2b). The extensive interactions explain the high affinity of Fab2838 (K_D = 4.4 nM) (Supplementary Fig. 8).

The Fab2838 CDR-H3 binding site in A_{2A}AR is similar to those for Nb80 CDR-3 in β_2AR[2] and for GαCT in opsin[1]. A critical difference is that Fab2838 stabilises an inactive conformation whereas the others recognise active conformations of the receptors. These structures are compared in Figure 3. In the opsin structure, GαCT, which forms a short α-helix, fits into a large pocket formed by helices II, III, V, VI, and VII interacting with the Arg residue of the D(E)RY motif in helix III (Fig. 3, left panels). CDR-3 of Nb80 in the β_2AR structure binds in a similar position to GαCT although CDR-3 forms a β-hairpin[1] (Fig. 3, middle panels). Interestingly, CDR-H3 of Fab2838 also forms a β-hairpin but induces a differently shaped binding-pocket (Fig. 3c). In the β_2AR structure, CDR-3 of Nb80 is positioned between helices III and VI, whereas in the A_{2A}AR structure CDR-H3 of Fab2838 is ~ 6 Å closer to helices II and VII (Fig. 3b and Supplementary Fig. 9). This allows the close association of helices III and VI and the formation of the modified 'ionic lock' between R102$^{3.50}$ in helix III and E228$^{6.30}$ in helix VI, consequently stabilising the inactive conformation. In the β_2AR-Gs protein complex structure, the C-terminal α-helix

(α5) of Gαs also binds in a similar position to CDR-H3[13] (supplementary Fig. 10). The conformational changes of α5 together with the Gαs N-terminal region induced by the activated receptor was proposed to lead a nucleotide exchange from GDP to GTP in Gαs and to subsequent dissociation of the subunit from the receptor[19]. Thus, the binding pocket formed by helices II, III, VI, and VII seems to be the key site for the signal transfer between GPCR and G-protein.

A possible inactivation mechanism of A_{2A}AR by Fab2838 is summarised as follows. Agonist binding induces large displacements of the intracellular ends of helices III, VI, and VII[16,17], which are essential to form the G-protein binding-pocket[13,19] (Supplementary Fig. 1). This indicates that the signal from the ligand-binding pocket is transferred through these helices and the conformations of the two pockets are strongly coupled. Our agonist and antagonist binding experiments indicate that this coupling also allows signal transfer in a reverse direction, from the G-protein binding to the ligand-binding pockets (Fig. 1). CDR-H3 of Fab2838 locks the positions of helices III, VI, and VII from the cytoplasmic side, leading to an inactive conformation of the extracellular ligand-binding pocket to which agonists cannot bind probably because of the rearrangement of the side chains at the bottom of the ligand-binding pocket including W246$^{6.48}$, the toggle switch for activation (for details, see Supplementary Fig. 1 and 11). A similar conceptual model on the β_2AR activation was reported by Kobilka, Sunahara, and colleagues[20]. In the case of β adrenergic receptors, the conformational coupling of the ligand and G-protein binding pockets seems less strict as demonstrated in the structures of β_1AR-agonist complexes[21] and β_2AR-irreversible agonist complex[22]. This may be because the A_{2A}AR and β_1/β_2AR agonists interact with different helices in the binding pockets (for details, see Supplementary Discussion).

Antibody fragments (and nanobodies) such as Nb80 and Fab2838 that recognise conformational epitopes of GPCRs have great potential for GPCR studies *in vitro* and *in vivo.* Although antibodies recognising the intracellular surface are not suitable for direct therapeutic use, the CDR structures should provide useful information to design peptides or small-molecule compounds against their clearly defined pockets to control the activation states of GPCRs. The antibody-fragments will be also useful tools to study ligand-binding kinetics of GPCRs because they can separate ligand-binding from equilibrium-shifts between different activation states of the receptors. Our approach based on the conventional mouse-hybridoma system allows us to raise antibodies against various receptors in 3-4 months using standard laboratory equipment.

METHODS SUMMARY

Expression and purification

$A_{2A}AR^{N154Q}$ (residues 1-316) was expressed in *P. pastoris* as described previously[23] and purified as described in Methods.

Antibody generation

MRL/lpr mice were immunised with the purified A_{2A}AR with the antagonist ZM241385. Antibodies were raised to recognise conformational epitopes of A_{2A}AR using the conventional mouse-hybridoma system[24] combined with new screening methods as described in Methods. The Fab fragments were obtained by papain cleavage and purified by anion-exchange column chromatography.

Crystallisation, data collection, and structure determination

Purified A_{2A}AR was mixed with the Fab fragment and the A_{2A}AR -Fab complex was purified twice by gel filtration chromatography. Crystals were grown by vapour diffusion under the conditions described in the Methods. Diffraction data were collected from a single cryo-cooled crystal on beamline I24 at the Diamond Light Source Ltd., UK. The structures were solved by molecular replacement using the receptor from the A_{2A}AR-T4L structure (PDB code, 3EML) and an antibody Fab-fragment structure (PDB code 1P7K) as search models. Data collection and refinement statistics are summarised in Supplementary Table 2.

Supplementary Material

Refer to Web version on PubMed Central for supplementary material.

Acknowledgments

This work was supported by a grant from the ERATO Human Receptor Crystallography Project from the Japan Science and Technology Agency, by the Targeted Proteins Research Program from the Ministry of Education, Culture, Sports, Science and Technology, and by Development of New Functional Antibody Technologies of the New Energy and Industrial Technology Development Organization (NEDO), Japan. It was also partly funded by the Biotechnology and Biological Sciences Research Council (BBSRC) (BB/G023425/1). The work was partly performed in the Membrane Protein Laboratory funded by the Wellcome Trust (grant 062164/Z/00/Z) at the Diamond Light Source Limited. Data were collected at Diamond Light Source ID24 with the assistance of the beam line scientists, Gwyndaf Evans, Robin Owen, Danny Axford and Jun Aishima.

APPENDIX

METHODS

Construction of A_{2A}AR expression vectors for *Pichia pastoris*

The coding sequence of A_{2A}AR from residues 1 to 316 including the N-terminal $\tilde{\alpha}$ factor, FLAG-tag sequence, and C-terminal His (10)-tag was synthesised by optimisation of codon usage for *P. pastoris* (TAKARA bio Inc.). In the construct, N154 was also replaced by Gln to eliminate N-linked glycosylation. The DNA fragment was inserted into the multiple cloning site of the pPIC9K vector, and the linearised vector was transformed into the *P. pastoris* strain SMD1163 (Invitrogen) as described previously[23]. The transformed cells were stored as glycerol stocks at −80°C.

Expression and purification of A_{2A}AR

A_{2A}AR was expressed in *P. pastoris* as described previously[23]. Cells were suspended in buffer A (50 mM Sodium Phosphate, 100 mM NaCl, 5% glycerol, 2 mM EDTA, protease inhibitor cocktail (Roche); pH 7.4) and disrupted with glass beads (0.5 mm Biospec) by vigorous agitation at 350 rpm for 2 h at 4°C. Following removal of unbroken cells and cell debris at 10,000 × *g*, membranes were isolated by ultracentrifugation at 100,000 × *g* for 45 min. Membranes were resuspended in buffer B (20 mM Hepes, 500 mM NaCl, 30 % glycerol, EDTA-free protease inhibitor cocktail (Roche); pH 7.0) and solubilised by 1% n-dodecyl β-D-maltoside (DDM; Anatrace) containing 0.2% cholesterol hemi succinate (CHS; Sigma) in the presence of 4 mM theophylline (antagonist) for 1-2 h at 4°C. After ultracentrifugation, the supernatant was supplemented with solid imidazole to a final concentration of 40 mM and incubated overnight with a TALON immobilised metal ion affinity chromatography resin (Clonetech) at 4°C with gentle rotation (1 mL of TALON resin/150 mg of total protein). The resin was washed with buffer C (20 mM Hepes, 250 mM NaCl, 10% glycerol, protease inhibitor cocktail, 0.05% DDM, 0.01% CHS; pH 7.0) containing 20 mM imidazole, and the bound A_{2A}AR was eluted with buffer C containing

300 mM imidazole. The purified sample was incubated overnight with ConA resin at 4°C to remove contaminating glycosylated proteins and was collected in the flow-through fraction. The final purified sample was dialysed against buffer C and concentrated to approximately 20 mg/mL by ultrafiltration (ULTRA-4 100 K, Millipore).

Construction, expression, and purification of A_{2A}AR-T4L

A_{2A}AR-T4L is a variant of A_{2A}AR in which the ICL3 region is replaced with a bacteriophage T4 lysozyme (T4L): N2 to Y161 of T4L were inserted between L208 and R222 within the ICL3 region replacing residues K209 to A221. A_{2A}AR-T4L was expressed in *P. pastoris* and purified as described above.

Antibody generation

All animal experiments described in this study conformed to the guidelines outlined in the Guide for the Care and Use of Laboratory Animals of Japan and were approved by the University of Tokyo Animal Care Committee (approval no. RAC07101). To raise antibodies against conformational epitopes of A_{2A}AR, we modified existing protocols for immunisation and screening of mouse monoclonal antibodies. A detailed description of these modified protocols will be published elsewhere. Briefly, MRL/lpr mice were immunised with 0.1 mg purified A_{2A}AR-antagonist ZM241385 complex 3 times with 2 week intervals. The immunised mice were sacrificed and single cell suspensions were prepared from the spleen. These cells were fused with NS-1 myeloma cells using polyethylene glycol (PEG) according to conventional methods[24]. Primary screening of hybridoma culture supernatants was performed using the liposome ELISA assay. To screen antibodies that specifically recognise native receptors, we developed a novel ELISA method using proteoliposomes. For 'liposome-ELISA', we used purified A_{2A}AR reconstituted into liposomes containing biotinyl phosphatidylethanolamine (Avanti) to maintain the protein in its native conformation and effectively immobilise liposomes onto streptavidin-coated plates (Nunc). To eliminate antibodies recognising flexible loops, N (and C)-termini or unstructured regions of A_{2A}AR, we performed ELISA using A_{2A}AR denatured with 1% sodium dodecyl sulphate. Denatured ELISA-negative cells were collected and evaluated using a BIAcore T100 (GE Healthcare) as described below. The selected cells were isolated by limiting dilution to establish monoclonal hybridoma cell lines producing antibodies against A_{2A}AR. For large-scale antibody production, the monoclonal hybridoma cells were inoculated into BALB/c athymic nude mice. IgG was collected from mouse ascites fluid by precipitating twice with 50% ammonium sulphate and purified using Melon Gel (Thermo) according to the manufacturer's protocol. Fab fragments were obtained by proteolytic cleavage of IgG with papain (Worthington) and purified by anion-exchange column chromatography (DEAE 5-PW, TOSOH). The sequences of Fab fragments were determined according to the standard 5′-RACE method using total RNA isolated from hybridoma cells.

Binding assay by surface plasmon resonance

The BIAcore T100 system and reagents, including sensor chips and amine coupling kit, were obtained from GE Healthcare. Monoclonal anti-mouse Fc antibody (200 μg/mL; Millipore) was immobilised on a CM5 sensor chip using the amine coupling kit according to the manufacturer's instructions. Antibodies in hybridoma culture supernatants (50 μL) or purified monoclonal antibodies (50 μg/mL) were tightly trapped by the Fc-antibody fixed on the sensor chip. The antibodies bound tightly so as not to be released from the surface when washing with buffer D (20 mM Hepes, 100 mM NaCl, 0.05% DDM, 0.01% CHS; pH 7.0). Purified A_{2A}AR (or A_{2A}AR-T4L) was passed over the surface and the specific binding was monitored for 2 min at 20°C. Subsequently, the sensor surface was washed with buffer D and the dissociation was monitored for 6 min at 20°C. Association and dissociation rate constants (k_{on} and k_{off}) were determined using a curve-fitting protocol as implemented in

the BIAevaluation software (Version 1.1, GE Healthcare) based on the Langmuir isotherm model assuming 1:1 binding stoichiometry.

Ligand binding assays

Ligand binding assays were performed using radioligands of the antagonist [^{3}H]-ZM241385 and the agonist [^{3}H]-NECA (GE Healthcare). For single-point binding assays, 5 nM [^{3}H]-ZM241385 or 5 μM [^{3}H]-NECA was incubated in 50 μL of buffer D containing 5 nM or 50 nM purified A_{2A}AR with or without 500 nM antibody for 1 h on ice. For saturation-binding assays, varying concentrations of [^{3}H]-ZM241385 or [^{3}H]-NECA were incubated in 50 μL of buffer D containing 5 nM or 50 nM purified A_{2A}AR with or without 500 nM antibody (Fab2838) for 1 h on ice. Receptor-bound ligands were separated by gel filtration[25] and radioactivity was measured using a LS6500 scintillation counter (Beckman). Data were analysed by a nonlinear-regression-fitting program using the GraphPad Prism software. Competition assays with antagonists (SCH442416, theophylline) and agonists (NECA, adenosine) were performed in the presence of 1.0 nM [^{3}H]-ZM241385 for A_{2A}AR or 1.5 nM for A_{2A}AR-Fab (corresponding to the respective K_Ds).

Purification and crystallisation of the A_{2A}AR-Fab complex

Purified A_{2A}AR and the Fab fragments were mixed at 1:1.2 molar ratio and were incubated on ice for 1 h. The mixture was loaded onto a Superdex 10/300 column (GE Healthcare) equilibrated with buffer C and eluted using the same buffer. The gel filtration step was repeated twice to ensure successful crystallisation of the A_{2A}AR-Fab complex. Fractions containing the complex were concentrated to approximately 20 mg/mL by ultrafiltration (ULTRA-4 100 K, Millipore). Initial crystals were obtained using MemGold (Molecular Dimensions Ltd.). After optimisation, well-diffracting crystals were obtained in hanging drops by vapour diffusion at 20°C with the protein solution containing 0.3-0.6% octyl-thioglucoside and the reservoir solution (1 μL) containing 30% PEG400, 0.1 M MES (pH 6.5) and 0.2 M $MgCl_2$. Crystals appeared after 1 day and grew to maximum dimensions in 1 week before being flash-frozen and stored in liquid nitrogen.

Data collection and structure determination

Diffraction data were collected from single cryo-cooled crystals (100K) on beamline I24 at Diamond Light Source Ltd., UK using a 10-μm focused beam (wavelength 0.9795 Å) and a pilatus 6 M detector (Dectris Ltd., Switzerland). Data were processed using MOSFLM and SCALA from the CCP4 program suite[26]. The structure was initially solved using the 2.7 Å data. Molecular replacement was carried out with PHASER[27] using the receptor from the A_{2A}AR-T4 lysozyme fusion structure (PDB code 3EML) and an antibody fragment (PDB code 1P7K) as search models. Iterative cycles of model building and structure refinement were performed using Coot[28], Refmac5[29] and phenix.refine in the PHENIX program package[30]. The final model from this refinement was used as the initial model for refinement against the 3.1 Å data. The refinement was carried out similarly to above. Model validation was performed using Procheck[31] and MolProbity[32]. The resulting crystallographic and refinement statistics are summarised in Supplementary Table 2. Disordered region of A_{2A}AR was predicted by the RONN program[33]. Figures were prepared using PyMOL (The PyMOL Molecular Graphics System, Version 1.3, Schrodinger, LLC.).

References

25. Warne T, Chirnside J, Schertler GFX. Expression and purification of truncated, non-glycosylated turkey beta-adrenergic receptors for crystallization. Biochim. Biophys. Acta. 2003; 1610:133–140. [PubMed: 12586387]

26. Collaborative Computational Project. N. The CCP4 suite: programs for protein crystallography. Acta Crystallogr. D. 1994; 50:760–763. [PubMed: 15299374]
27. McCoy AJ, et al. Phaser crystallographic software. J. Appl. Crystallogr. 2007; 40:658–674. [PubMed: 19461840]
28. Emsley P, Cowtan K. Coot: model-building tools for molecular graphics. Acta Crystallogr. D. 2004; 60:2126–2132. [PubMed: 15572765]
29. Murshudov GN, Vagin AA, Dodson EJ. Refinement of macromolecular structures by the maximum-likelihood method. Acta Crystallogr. D. 1997; 53:240–255. [PubMed: 15299926]
30. Afonine PV, Grosse-Kunstleve RW, Adams PD. A robust bulk-solvent correction and anisotropic scaling procedure. Acta Crystallogr. D. 2005; 61:850–855. [PubMed: 15983406]
31. Laskowski RA, MacArthur MW, Thornton JM. Validation of protein models derived from experiment. Curr. Opin. Struct. Biol. 1998; 8:631–639. [PubMed: 9818269]
32. Chen VB, et al. MolProbity: all-atom structure validation for macromolecular crystallography. Acta Crystallogr. D. 2010; 66:12–21. [PubMed: 20057044]
33. Yang ZR, Thomson R, McNeil P, Esnouf RM. RONN: the bio-basis function neural network technique applied to the detection of natively disordered regions in proteins. Bioinformatics. 2005; 21:3369–3376. [PubMed: 15947016]

References

1. Scheerer P, et al. Crystal structure of opsin in its G-protein-interacting conformation. Nature. 2008; 455:497–502. [PubMed: 18818650]
2. Rasmussen SGF, et al. Structure of a nanobody-stabilized active state of the β2 adrenoceptor. Nature. 2011; 469:175–180. [PubMed: 21228869]
3. Palczewski K, et al. Crystal structure of rhodopsin: A G protein-coupled receptor. Science. 2000; 289:739–745. [PubMed: 10926528]
4. Shimamura T, et al. Crystal structure of squid rhodopsin with intracellularly extended cytoplasmic region. J. Biol. Chem. 2008; 283:17753–17756. [PubMed: 18463093]
5. Murakami M, Kouyama T. Crystal structure of squid rhodopsin. Nature. 2008; 453:363–367. [PubMed: 18480818]
6. Warne T, et al. Structure of a beta1-adrenergic G-protein-coupled receptor. Nature. 2008; 454:486–491. [PubMed: 18594507]
7. Rasmussen SGF, et al. Crystal structure of the human beta2 adrenergic G-protein-coupled receptor. Nature. 2007; 450:383–387. [PubMed: 17952055]
8. Cherezov V, et al. High-resolution crystal structure of an engineered human beta2-adrenergic G protein-coupled receptor. Science. 2007; 318:1258–1265. [PubMed: 17962520]
9. Jaakola V-P, et al. The 2.6 angstrom crystal structure of a human A2A adenosine receptor bound to an antagonist. Science. 2008; 322:1211–1217. [PubMed: 18832607]
10. Wu B, et al. Structures of the CXCR4 Chemokine GPCR with Small-Molecule and Cyclic Peptide Antagonists. Science. 2010; 330:1066–1071. [PubMed: 20929726]
11. Shimamura T, et al. Structure of the human histamine H1 receptor complex with doxepin. Nature. 2011; 475:65–70. [PubMed: 21697825]
12. Chien EYT, et al. Structure of the Human Dopamine D3 Receptor in Complex with a D2/D3 Selective Antagonist. Science. 2010; 330:1091–1095. [PubMed: 21097933]
13. Rasmussen SGF, et al. Crystal structure of the β2 adrenergic receptor-Gs protein complex. Nature. 2011; 477:549–555. [PubMed: 21772288]
14. Fredholm BB, Chen JF, Masino SA, Vaugeois JM. Actions of adenosine at its receptors in the CNS: insights from knockouts and drugs. Annu. Rev. Pharmacol. Toxicol. 2005; 45:385–412. [PubMed: 15822182]
15. Müller CE, Jacobson KA. Recent developments in adenosine receptor ligands and their potential as novel drugs. Biochim. Biophys. Acta. 2011; 1808:1290–1308. [PubMed: 21185259]
16. Xu F, et al. Structure of an Agonist-Bound Human A2A Adenosine Receptor. Science. 2011; 332:322–327. [PubMed: 21393508]

17. Lebon G, et al. Agonist-bound adenosine A(2A) receptor structures reveal common features of GPCR activation. Nature. 2011; 474:521–525. [PubMed: 21593763]
18. Doré AS, et al. Structure of the adenosine A(2A) receptor in complex with ZM241385 and the xanthines XAC and caffeine. Structure. 2011; 19:1283–1293. [PubMed: 21885291]
19. Chung KY, et al. Conformational changes in the G protein Gs induced by the β2 adrenergic receptor. Nature. 2011; 477:611–615. [PubMed: 21956331]
20. Yao XJ, et al. The effect of ligand efficacy on the formation and stability of a GPCR-G protein complex. Proc. Natl Acad. Sci. USA. 2009; 106:9501–9506. [PubMed: 19470481]
21. Warne T, et al. The structural basis for agonist and partial agonist action on a beta(1)-adrenergic receptor. Nature. 2011; 469:241–244. [PubMed: 21228877]
22. Rosenbaum DM, et al. Structure and function of an irreversible agonist-beta(2) adrenoceptor complex. Nature. 2011; 469:236–240. [PubMed: 21228876]
23. Yurugi-Kobayashi T, et al. Comparison of functional non-glycosylated GPCRs expression in Pichia pastoris. Biochem. Biophys. Res. Commun. 2009; 380:271–276. [PubMed: 19167344]
24. Köhler G, Milstein C. Continuous cultures of fused cells secreting antibody of predefined specificity. Nature. 1975; 256:495–497. [PubMed: 1172191]

Europe PMC Funders Author Manuscripts

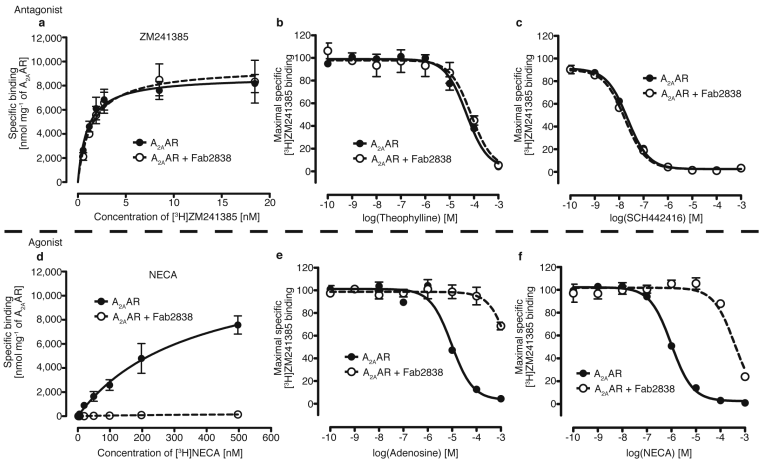

Figure 1. Effect of Fab2838 on A_{2A}AR -ligand binding

a, Saturation binding curves for an antagonist [^{3}H]-ZM241385 binding to A_{2A}AR with (open circle) or without (closed circle) Fab2838. **b** and **c**, Inhibition of [^{3}H]-ZM241385 binding by the antagonists, theophylline (**b**) and SCH442416 (**c**) with (open circles) and without (closed circles) Fab2838. The binding of [^{3}H]-ZM241385 in the absence of competitor was set at 100%. **d,** Similar to **a**, but for the agonist [^{3}H]-NECA. **e** and **f**, Similar to **c** and **d** but for the agonists, adenosine (**e**) and NECA (**f**), respectively. All data are the mean ± standard estimated errors (SEM) of three independent experiments performed in duplicate.

Europe PMC Funders Author Manuscripts

Europe PMC Funders Author Manuscripts

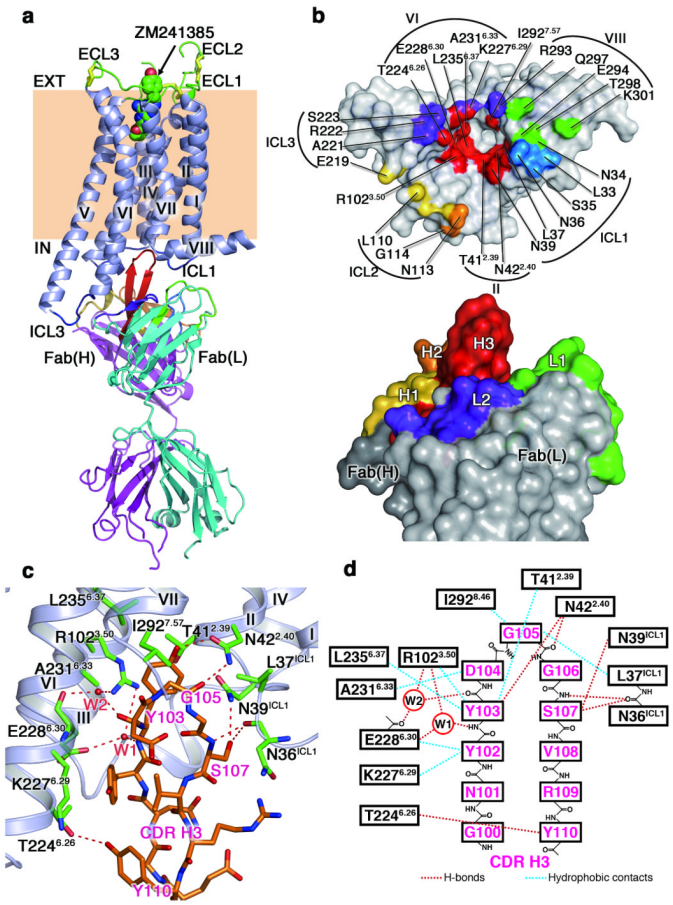

Figure 2. Structure of the A_{2A}AR complex with an antibody Fab2838 fragment

a, Overall structure viewed parallel to the membrane. A_{2A}AR and the Fab light and heavy chains are shown in blue-grey, cyan, and magenta, respectively. The three disulfide bonds in the ECLs are represented by yellow sticks. The bound antagonist ZM241385 in the ligand-binding pocket is shown as a space-filling model. The complementarity-determining regions (CDRs) of Fab2838 are as follows: CDR-H1, yellow; CDR-H2, orange; CDR-H3, red; CDR-L1, green; CDR-L2, purple; CDR-L3, marine. **b**, Surface representation of the interface between A_{2A}AR (top) and Fab2838 (bottom). Compared to **a**, A_{2A}AR has been rotated 90° around a horizontal axis, whereas Fab2838 is shown in the same orientation. **c**, View of the A_{2A}AR (green residues) and CDR-H3 (orange residues) interface. Red dotted lines indicate polar interactions. **d**, Schematic representation of the A_{2A}AR and CDR-H3 interface.

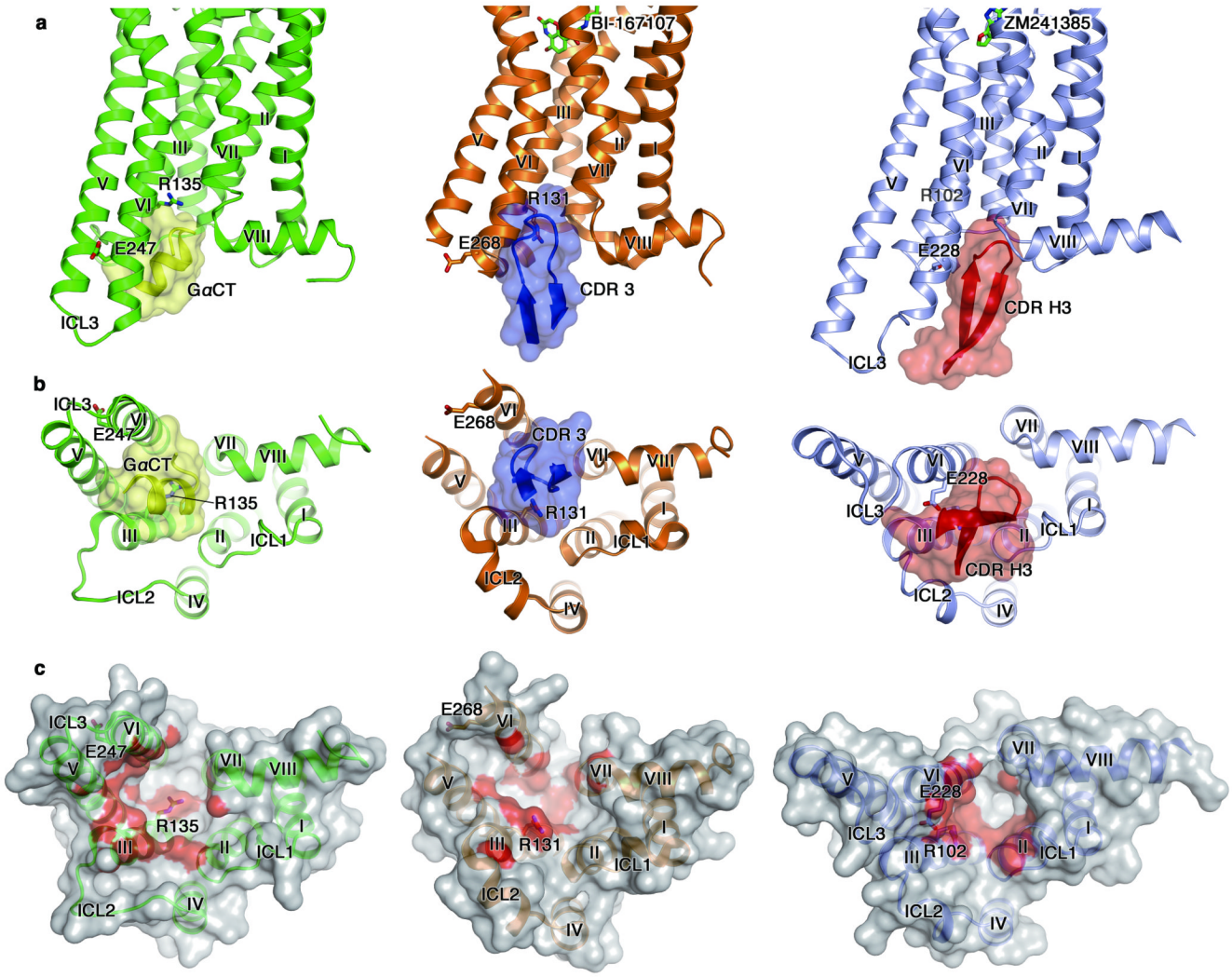

Figure 3. Comparison of the structures of opsin-GαCT, β2AR-Nb80 and A_{2A}AR-Fab2838 complexes

Left, middle and right panels show the structures of an active form of opsin with GαCT (opsin in green and GαCT in yellow), an active form of β_2AR with Nb80 CDR-3 (β_2AR in brown and Nb80 CDR-3 in blue) and an inactive form of A_{2A}AR with Fab2838 CDR-H3 (A_{2A}AR in blue-grey and Fab2838 CDR-H3 in red). **a**, Views parallel to the membrane. Bound ligands are shown as stick models in β_2AR and A_{2A}AR. The residues involved in the 'ionic lock' formation are also shown. Nitrogen and oxygen atoms are in blue and red, respectively. **b**, Cytoplasmic views of the complexes. **c**, Surface representations of cytoplasmic surfaces of the receptors. Surfaces within 4 Å of GαCT/CDR-3/CDR-H3 are red.

Europe PMC Funders Author Manuscripts